This manuscript has yet to be reviewed. Subsequent versions may have different content. Please feel free to contact the corresponding author, Anson Mackay, as I'd welcome any feedback.

Neoglacial trends in diatom dynamics from a small alpine lake in the Qinling Mountains of central China.

Bo Cheng[1], Jennifer Adams[2], Jianhui Chen[3], Aifeng Zhou[3], Qing Zhang[3], Anson Mackay[4*]

[1]Bo Cheng,
College of Urban and Environmental Science, Central China Normal University,
Wuhan 430079 China
chengbo@mail.ccnu.edu.cn

[2]Jennifer Adams
Department of Earth Sciences, University of Toronto, Toronto, ON, Canada
j.adams@utoronto.ca

[3]JianHui Chen
Key Laboratory of West China's Environmental System (Ministry of Education), College of Earth and Environmental Sciences, Lanzhou University, Lanzhou 730000 China
jhchen@lzu.edu.cn

[3]Aifeng Zhou,
Key Laboratory of Western China's Environmental Systems (Ministry of Education), College of Earth and Environmental Sciences, Lanzhou University, Lanzhou 730000, China
zhouaf@lzu.edu.cn

[3]Qing Zhang,
Key Laboratory of Western China's Environmental Systems (Ministry of Education), College of Earth and Environmental Sciences, Lanzhou University, Lanzhou 730000, China
Zhangqing16@lzu.edu.cn

[4]Anson Mackay*
ECRC, Department of Geography, UCL, London WC1E 6BT UK
ans.mackay@ucl.ac.uk
Corresponding Author

Authors have no competing interests to declare

Abstract:

During the latter stages of the Holocene, and prior to anthropogenic global warming, the Earth underwent a period of cooling called the neoglacial. The neoglacial was associated with declining summer insolation and changes to Earth surface albedo. Although impacts varied globally, in China the neoglacial was generally associated with cooler, more arid climate, which led to renewed permafrost formation, and shifts in vegetation composition. Few studies in central China, however, have explored the impact of neoglacial cooling on freshwater diversity, especially in remote alpine regions. Here we take a palaeolimnological approach to characterise multidecadal variability in diatom community composition, beta-diversity, and flux-inferred productivity over the past 3,500 years in the Qinling Mountains, biodiversity hotspot. We investigate the impact of long-term cooling on primary producers in an alpine lake, which are fundamental to overall aquatic ecosystem function. We show that trends in beta-diversity and shifts in ecological guilds likely reflect changing lake-catchment resource availability, linked to both long-term attenuation of the Asian summer monsoon, and abrupt cool events, linked to a strengthened Siberian High. Important diatom community and productivity responses to the Medieval Climatic Optimum and the Little Ice Age are all apparent in our record, although impact from previous centennial-scale, cool-events are less evident.

Keywords:

Diatoms, beta-diversity, Qinling Mountains, neoglacial

1. Introduction

Alpine freshwaters have multiple ecosystem functions (Messerli et al. 2004; Buytaert *et al.,* 2017) and provide many ecosystem services such as freshwater regulation and habitat provision (Grêt-Regamey et al. 2011). Their multifunctionality depends on local species assemblages, and how they vary through space and time, i.e. beta-diversity (Mori *et al.* 2018). Beta-diversity links biodiversity at regional and local scales, and the amount of compositional change over time can provide important indications about ecosystem functioning (Birks 2007). For example, estimating species turnover assumes that species are lost and gained over time in response to resource availability, competition, historical events and environmental factors such as climate change, over both recent (Smol et al. 2005) and long timescales (Leprieur et al. 2011). However, Alpine regions around the world are some of the most sensitive to changing climate, due in part to elevation-dependent warming (Pepin et al. 2015). Elevation-dependent warming in recent decades across sites on the Tibetan Plateau, for example, showed some of the greatest changes globally (Yan and Liu 2014). Understanding how high altitude ecosystems respond to changing climate is a matter of urgency, because not only do these regions act as 'water towers' supplying water to huge populations downstream (Messerli et al. 2004; Buyteart *et al.,* 2017), but their habitats to many iconic species are also vulnerable (e.g. Fan et al. 2014).

Natural archives are an important resource for reconstructing past environments where long-term records are either scarce or absent. In central China, speleothems provide exceptional, high resolution records of monsoon intensity, allowing periods of multiannual and multidecadal drought to be determined (Wang et al. 2005). Yet there are relatively few studies (e.g. Liu et al. 2017) which have explored multidecadal records of biodiversity change over similar timescales, leaving a fundamental gap in understanding as to how biodiversity in freshwater ecosystems, especially at higher altitudes, responded to periods of

99 climate variability. Reconstructing the impacts of past climate on freshwater ecosystems is
100 fundamental to understanding how freshwater biodiversity may respond to future climate,
101 especially during periods of rapid change. Here we focus on the neoglacial, which spans at
102 least the past c. 3,500 years.
103
104 The neoglacial, characterised by increasingly cooler temperatures, follows on from global
105 warmth of the early- to mid-Holocene. The extent of cooling varied regionally; it was very
106 pronounced in the extra-tropical northern hemisphere, but was less monotonic at low
107 latitudes (Marcott et al. 2013). The most important driver of northern hemisphere cooling is
108 declining summer insolation in conjunction with changes in albedo on the Earth's surface,
109 linked to feedbacks from vegetation and snow-ice albedo. In China, the neoglacial resulted
110 in the persistent decline in monsoon intensity in southern China (Wang et al. 2005) and rapid
111 decline in precipitation in northern China (Chen et al. 2015a) leading to increased aridity and
112 major shifts in vegetation communities (Zhou et al. 2010). Superimposed on the insolation-
113 driven neoglacial were notable periods of sub Milankovitch, centennial-scale climatic events
114 (e.g. Mayewski et al. 2004; Mann et al. 2009; Wanner et al. 2014), including the 2,800 yr BP
115 event (Hall et al. 2004), the Medieval Climactic Anomaly (c. 1000-1300 AD) and Little Ice
116 Age (c. 1300 – 1850 AD). The latter two events are well expressed throughout China;
117 Medieval temperatures were generally warmer than the following centuries spanning the LIA
118 (Cook et al. 2013; Chen et al. 2015b). However, while the LIA generally resulted in periods
119 of aridity (e.g. Wang et al. 2005; Tan et al. 2011; Chen et al. 2015a), in depth research
120 highlights a more heterogenous response across China (e.g. Cook et al. 2010), with some
121 central and southern regions becoming wetter due to interplays between the Westerly jet
122 stream and the ASM (Tan et al. 2018).
123
124 Freshwater ecosystems in the Qinling Mountains of central China provide natural capital and
125 ecosystem services for local and regional populations, and understanding the impact of
126 monsoon variability on ecosystem functioning has the potential to add insight into how

freshwater biodiversity may respond to future climate change, and predicted increases in mean annual precipitation (Guo et al. 2017). In this study, we investigate the effects of long-term climate change on freshwater biodiversity in an alpine lake situated in the Qinling mountain range, central China. Specifically we reconstruct trends in diatom community composition, their ecological guilds, and compositional turnover (beta-diversity) at a multidecadal resolution (c. 55 yrs) over the past 3500 years, to determine how primary producers have responded to neoglacial climate change and changing resource availability. We hypothesise that neoglacial cooling would result in a decline in available resources, and with it a decline in diatom beta-diversity.

1.1 Study region

The Qinling Mountains are widely recognised as a biodiversity hotspot (Fan et al. 2014; Zhang et al. 2017). The region is climatically very sensitive, as it separates the northern subtropical zone of China from the country's central warm-temperate zone (Figure 1). Mount Taibai (34°N, 108°E; 3767 m), is the highest mountain in the range, with a timberline at c. 3,370 m, and treeline at c. 3,600 m (Liu et al. 2002). The mountain is classified as a glacial heritage site because Quaternary glaciations are well preserved, especially the last glaciation (Yang et al. 2018). On Mount Tabai there are several clusters of cirque lakes, and our study site, Lake Yuhuang Chi (YHC), is found in one of these clusters. It is a cirque and moraine lake at 3370 masl, with a maximum depth of 21.5m and an area of c. 23,600 m^2. Its location places it in the *Larix* forest - subalpine meadow ecotone, making the lake – catchment ecosystem very sensitive to changes in climate.

Figure 1: Regional position of Lake Yuhuang Chi in the Qinling Mountains of central Asia. The lake is situated 3365m asl, and was formed by glacial activity. The photograph of the frozen lake to the right shows the small catchment and tundra vegetation.

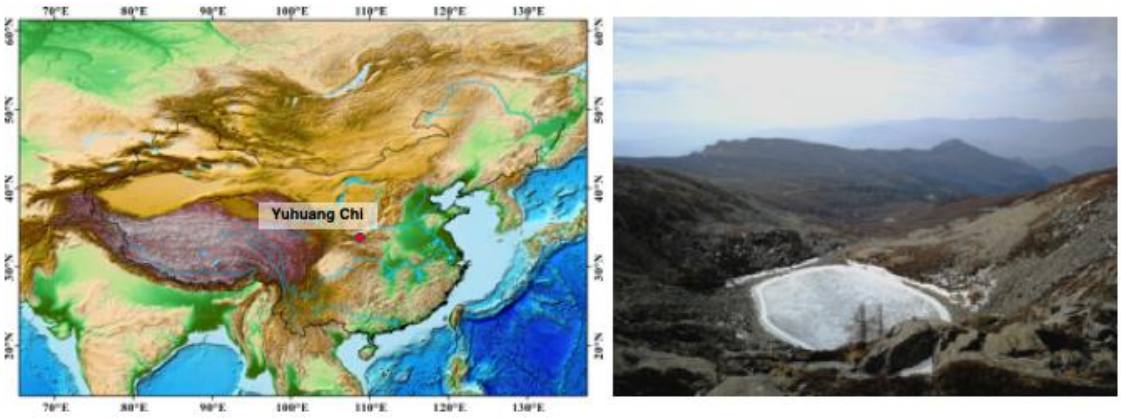

2. Methods:

2.1 Coring, Age model

A 135 cm sediment core (YHC15A) was collected using a 6cm diameter piston corer from the central region of Lake Yuhuang Chi. The core consisted entirely of grey-brown gyttja. Radiocarbon dating was carried out on bulk organic sediments using accelerator mass spectrometry (AMS) at Beta Analytic. There is a radiocarbon reservoir effect evident in the data, so we used a quadratic extrapolation to determined reservoir ages. All the radiocarbon dates were quadratic fitted (^{14}CAge = 0.0693depth^2 + 17.31depth + 1340, R^2 = 0.9994), so we determined the top (0cm) with a 1340 year reservoir age effect. An age-depth model was developed with smooth fit using CLAM 2.2 (Blaauw, 2010) in *R*, using Intcal13 (Reimer et al., 2013) calibration curve.

2.2 Diatoms

Diatom analysis was performed on alternate sediment samples, at a resolution of c. every 55 years. Approximately 0.1g of wet sediment from each sample was prepared using standard procedures. Organic matter was removed by heating each sample in 30% H_2O_2, before 10% HCl was added to remove carbonates and any excess H_2O_2. Diatom concentrations were

174 calculated through the addition of bivinylbenzene (DVB) microspheres (concentration 8.02 x
175 10^5 spheres/cm^2) to diatom suspensions, and diatom fluxes calculated using sediment
176 accumulation rates. Diatom suspensions were diluted such that suitable concentrations
177 could be calculated and then pipetted onto coverslips to dry before being fixed onto
178 microscope slides with Naphrax. Using a Zeiss Axiostar Plus light microscope, diatoms were
179 counted at x1000 magnification under an oil-immersion objective and phase contrast. A
180 minimum of 300 diatom valves were counted for each sample (min 331, max 591). Diatoms
181 were identified using a variety of flora including Krammer and Lange-Bertalot, 1986, 1988,
182 1991a, 1991b; Williams and Round, 1987; Lange-Bertalot, 2001.
183
184 Diatom species were categorised according to ecological guilds commonly associated with
185 the abundance of available resources (e.g. light, nutrients) and disturbance (e.g. grazing)
186 (after Passy 2007; Rimet & Bouchez 2012). The low profile guild includes diatoms which
187 attach themselves to substrates in erect, prostrate, & adnate forms, are very slow moving
188 (Passy 2007), and are generally adapted to low nutrient conditions. High profile guild
189 diatoms are those of tall stature (e.g. they are filamentous, or chain-forming, or found in
190 mucilage tubes), and are generally adapted to high nutrients and low levels of disturbance
191 (Passy 2007). Motile diatoms are relatively fast moving species, tolerant of high nutrients
192 (Passy 2007). A new planktic guild was determined by Rimet & Bouchez (2012) which
193 includes centric species able to resist sedimentation in lake ecosystems.
194
195 **2.3 Multivariate analyses**
196 The magnitude of diatom turnover was initially estimated using detrended correspondence
197 analysis (DCA), with square root transformation of the species data to stabilise variance and
198 rare species downweighted. The axis 1 gradient length was 1.44 standard deviation units, so
199 diatom abundances were reanalysed using principal components analysis (PCA). A log-
200 linear contrast PCA was undertaken, with symmetric scaling of ordination scores so that
201 scaling of both samples and species were optimised. A log-linear contrast PCA was also

undertaken for taxa grouped into genera. Beta-diversity, or species compositional change, was estimated using detrended canonical correspondence analyses (DCCA), with the diatom data constrained using dates from the calibrated age model (e.g. see Smol et al. 2005). We used DCCA to estimate beta-diversity because sample scores are scaled to be standard units of compositional turnover through the process of detrending by segments and non-linear rescaling (Birks 2007). Sample scores can therefore be interpreted as the amount of species turnover through time, making them ecologically useful and ideal for estimating compositional turnover. Ordinations was undertaken using Canoco5 (Šmilauer & Lepš 2014). Breakpoint analysis, a form of segmented regression analysis was used to determine major points of change in diatom composition, beta-diversity using the segmented package in R v. 3.5.1 (Muggeo 2008). Stringent p-values were adopted ($p<0.001$) when determining any major changes observed. All stratigraphical profiles shown were constructed using C2 Data Analysis Version 1.7.2, and zones determined using stratigraphical constrained cluster analysis by incremental sum of squares (CONISS) and broken stick analysis using the rioja package in R v. 3.5.1 (Juggins 2017).

3. Results

3.1 Age Model

Table 1: AMS-^{14}C radiocarbon dates from Lake Yuhuang Chi (core YHC15A)

Lab No.	Depth (cm)	Material	$\delta^{13}C$ (‰ VPDB)	^{14}C date ±error (yr BP)	^{14}C date minus 1340 reservoir age(yr BP)	Weighted calibrated age（No error） (yr BP)
Beta-425231	10	Bulk organic	-24.6	1530±30	190±30	168
Beta-425232	30	Bulk organic	-24.7	1920±30	580±30	595
Beta-425233	50	Bulk organic	-24.9	2370±30	1030±30	949
Beta-417757	70	Bulk organic	-24.8	2870±30	1530±30	1423
Beta-425234	110	Bulk organic	-24.8	4140±30	2800±30	2868
Beta-417758	130	Bulk organic	-24.9	4730±30	3390±30	3584

Figure 2: The age model determined on 5 radiocarbon dates of organic bulk sediments from core YHC15A. The age-depth model was developed with smooth fitting using CLAM 2.2 (Blaauw, 2010).

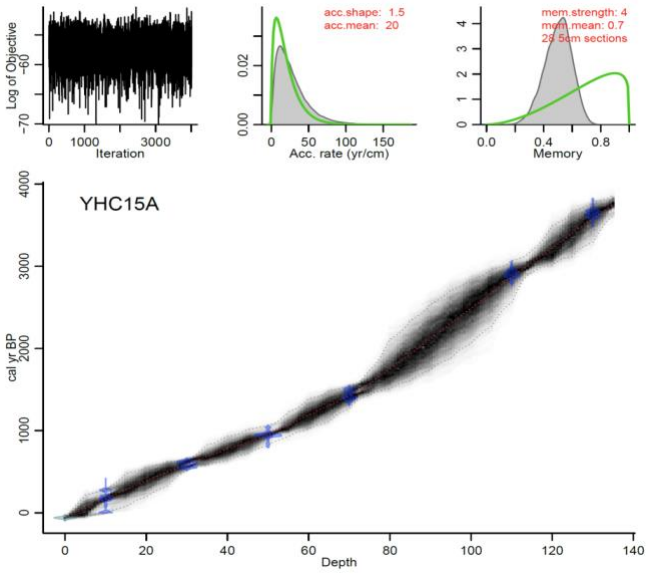

3.2 Diatoms

A total of 170 species of diatom were identified from Lake Yuhuang Chi, although by far the majority, 120 species, were rare (present < 1%). For much of the past 3,500 years, diatoms were dominated by fragilarioids and naviculoids up to c. 930 cal yrs BP, [1020 CE] after which they decline, to be replaced by monoraphid and *Gomphonema*-type taxa alongside the centric *Puncticulata*. Stratigraphically constrained cluster analysis by incremental sum of squares analyses (CONISS) on diatom relative abundance data reveals three zones. Zone 1 (c. 3550 – 2300 cal yrs BP), Zone 2 (c. 2300 – 615 cal yrs BP), and Zone 3 (c. 615 cal yrs BP – present) (Fig 3,4). Zone 1 is dominated by diatoms in the high profile guild (Fig 4), notably fragilarioids *Stauroforma exiguiformis* and *Staurosirella pinnata*. Diatoms in the motile guild are well represented by the naviculoid *Humidophila schmassmannii*, together with *Diadesmis gallica*, *Mayamaea atomus* and *Mayamaea fossalis*. The decline in *S. exiguiformis* at the top of the zone is accompanied by an increase in *Pseudostaurosira brevistriata*, and decline in motile diatoms e.g. *M. atomus*. In Zone 1, there is a gradual decline in beta-diversity, and decline in PCA1 samples scores. Zone 2 is marked by a notable increase in the planktic *Puncticulata bodanica* and increasing *P. brevistriata and Pseudostaurosira pseudoconstruens*. Diversity in zone 2 exhibits a rather stable, high profile flora, dominated by *P. brevistriata*, *P. pseudoconstruens* and *P. bodanica*, while *Gomphonema olivaceoides* and *Karayevia suchlandtii* appear in the record for the first time at c. 1400 and 1070 cal yrs BP, respectively. Motile diatoms become persistently lower than the mean at this time during zone 2, while low profile diatom abundances increase to fluctuate about the average (Fig 4). Zone 3 occurs just before a major change in diatom composition (PCA-1) and beta-diversity (Fig 3). Several species decline from the record altogether including *S. exiguiformis* and *H. schmassmannii*, while other species reach peak abundance for the whole profile, including *P. bodanica* and *G. olivaceoides*, and diatoms which occupy low profile guild status in general (Fig 4). *Denticula subtilis* appears in the record for the first time at c. 400 cal yrs BP. During zone 3, low profile and planktic diatoms increase to their highest values for the whole record, while profile diatoms are persistently

lower than the mean. Diatom fluxes range from 0.07 – 7.02 (mean 1.85) valves $x10^6$ cm^{-2} yr^{-1}. When centred around the mean, fluxes are highest in zone 2, between c. 1500 - 800 cal yrs BP (450 – 1150 CE), but decline at c. 800 cal yrs BP (1150 CE), to lowest values from c. 600 cal yrs BP (1350 CE) to the present (Fig 3).

Figure 3: Diatoms shown greater than 3% in more than one sample. Diatom species are given as relative abundances. Also shown are PCA axes 1 scores for species and genera, beta-diversity values, planktonic-benthic (P/B) ratio data, and mean-centred diatom fluxes. Zones were delimited using CONISS – see text for details. Red arrows delineate important breakpoints in data (where $p<0.001$). [see below]

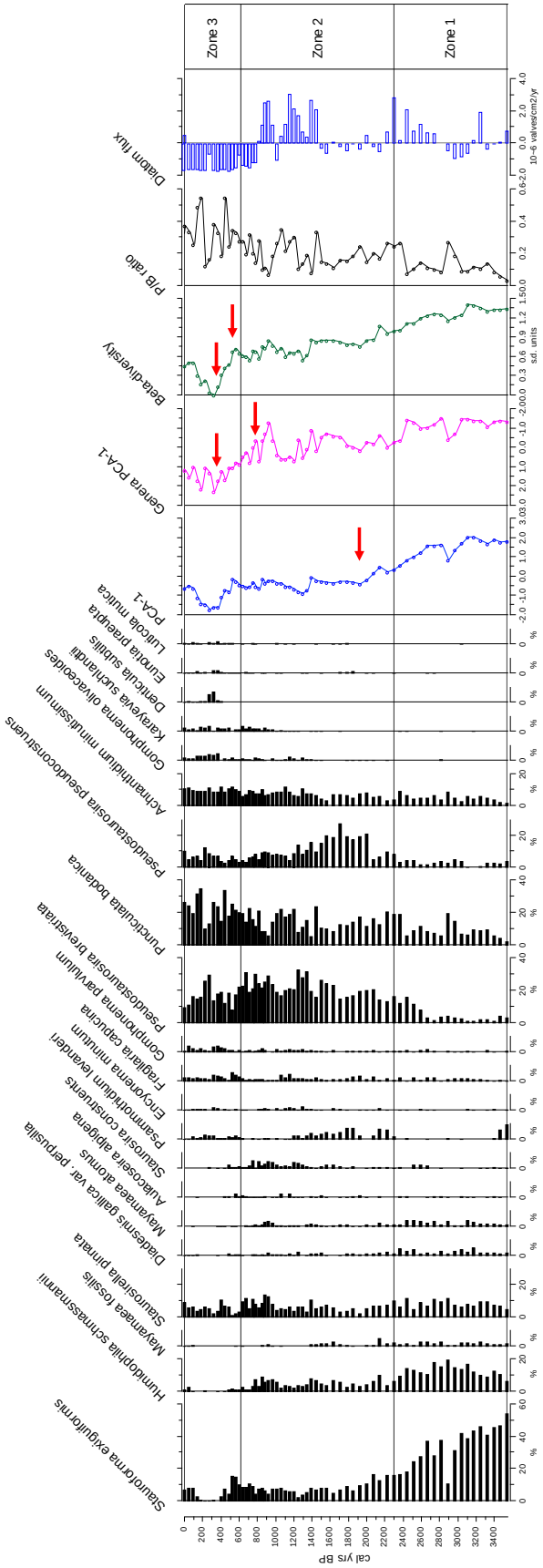
Zone 3
Zone 2
Zone 1
Diatom flux
10−6 valves/cm2/yr
P/B ratio
Bsea-diversity
sd. units
Scenea PCA-1
PCA-1
Lubcoa inulca
Eunotia praerupta
Denticula subtilis
Karayevia suchlandtii
Comptbonema olivaceoides
Achnanthidium minutissimum
Pseudostaurosira pseudoconstruens
Punctulata bodanica
Pseudostaurosira brevistriata
Gomphonema parvulum
Gomphonema capucina
Fragilaria capucina
Encyonema minutum
Psammothidium levanderi
Staurosira construens
Staurosira elliptica
Auliscoseira alomus
Mayamaea atomus var. perpusilla
Mayamaea gallica
Diadesmis gallica
Staurosirella pinnata
Mayamaea fossilis
Humidophila schmassmannii
Staurosirella exiguiformis
0
200
400
600
800
1000
1200
1400
1600
1800
2000
2200
2400
2600
2800
3000
3200
3400
cal yrs BP

Figure 4: All diatoms were classified into one of four guilds (after Passy 2007, and Rimet & Bouchez 2012): low profile (guild 1), high profile (guild 2), motile (guild 3) and planktic (guild 4). Guilds are presented as relative abundances to the left, and deviations around the mean to the right. Red arrows delineate important breakpoints in data (where p<0.001).

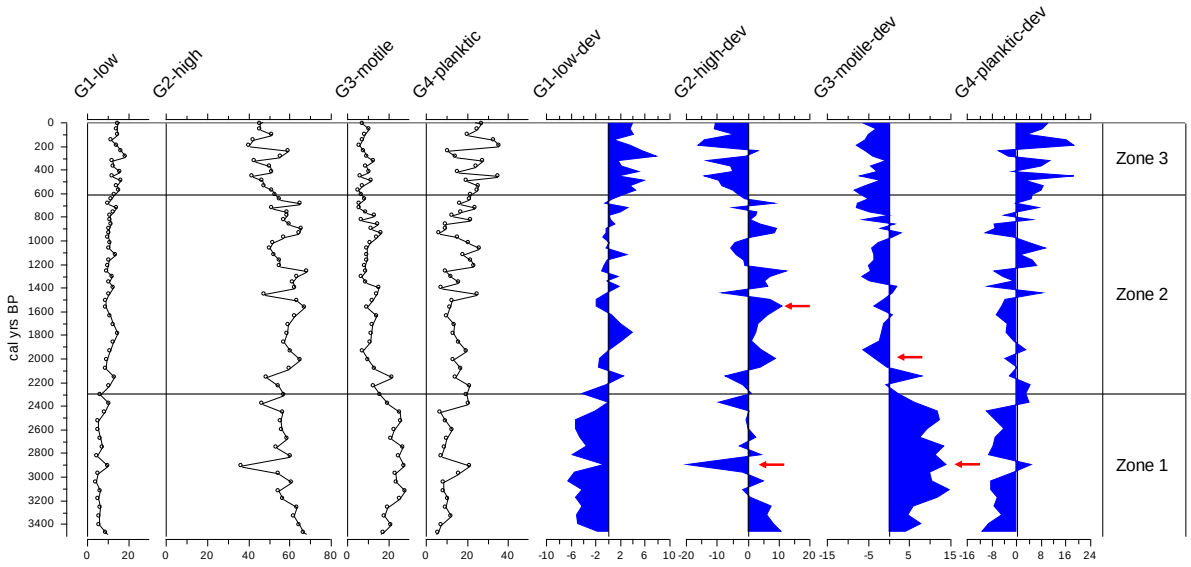

PCA highlights a very strong first axis gradient which accounts for over 45% of variation in the diatom data. Trends in PCA-1 are most clearly seen in Fig 5, as deviations around the mean. Breakpoint analysis indicates major (p<0.001) change in PCA axis 1 scores (Table 2), close to the transition when PCA values switch from being higher than the mean, to being lower than the mean, and low values persist for the rest of the record. Genera PCA axis 1 scores exhibit a permanent shift to lower-than-mean scores at c. 800 yrs BP (Fig 5). Beta-diversity (estimated from DCCA; 1.033 SD units) shows a similar pattern to PCA-1, with breakpoints identified at c. 515 cal yr BP ± 40 years, and 335 cal yr BP ± 33 years (Table 2; Fig 5).

Figure 5: Ordination and biodiversity trends shown as deviations around the mean. Red arrows delineate important breakpoints in data (where p<0.001).

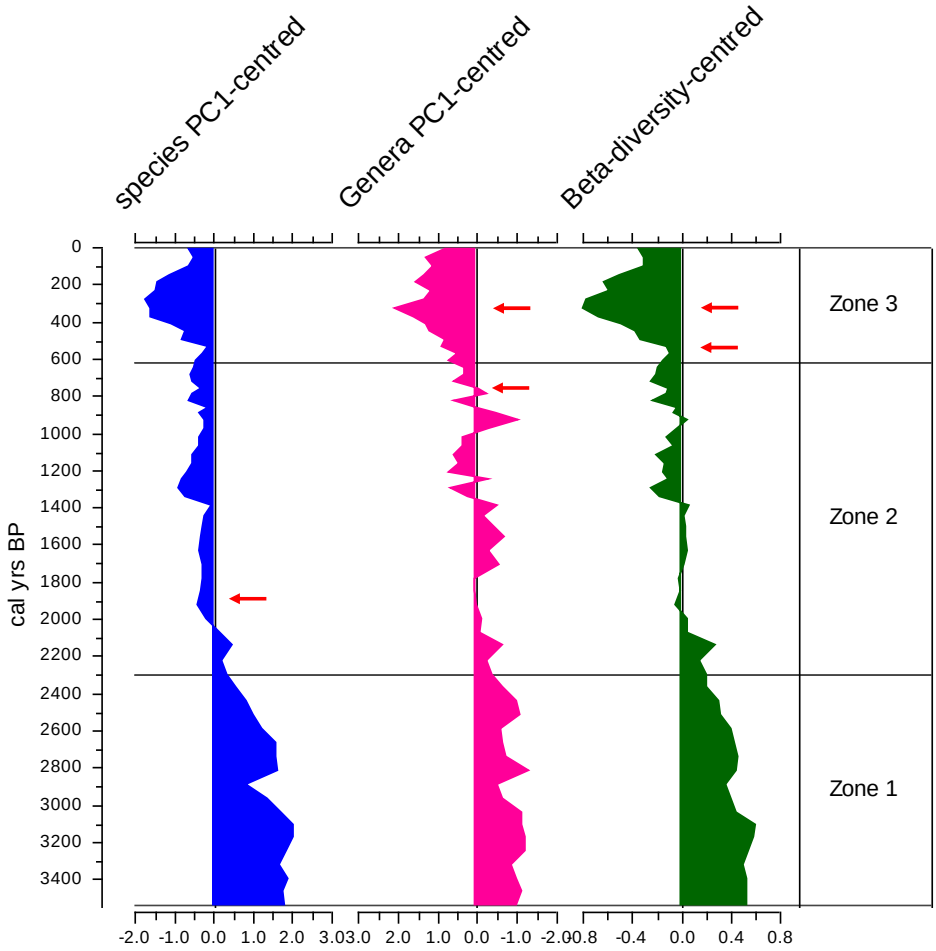

Table 2: Significant breakpoints in diatom trend data; p < 0.001).

	Breakpoint 1	p value	Breakpoint 2	p value
Species PCA	1850 BP ±200	p<0.001	none	
Genera PCA	760 BP (1190 CE) ± 85	p<0.001	330 BP (1620 CE) ± 70	p<0.001
Beta-diversity	515 BP (1435 CE) ± 97	p<0.001	335 BP (1615 CE) ± 33	p<0.001
Guild 2 – High profile	2910 BP ± 127	p<0.001	1565 BP ± 175	p<0.001
Guild 3 – Motile	2880 BP ± 69	p<0.001	1960 BP ± 128	p<0.001

4. Discussion:

4.1 Neoglacial trends in diatom diversity

For much of the past 3,500 years, the diatom flora in Lake Yuhuang Chi was dominated by species in the Fragilariaceae (Fig 3), which are common in high altitude lakes. Fragilarioids are often opportunistic, growing well in lakes with a short growing season and long periods of ice cover (e.g. Lotter & Bigler 2000). For example, July air temperature and ice cover duration have both been shown to have significant influence on fragilarioids in the European Alps (Schmidt et al. 2004), while in a sub-alpine lake in the Eastern Sayan mountains, insolation and northern hemisphere air temperatures played a strong role on modulating fragilarioid responses through the Holocene (Mackay et al. 2012). The abundant, high profile species *S. exiguiformis*, is common in dystrophic lakes, which have high concentrations of humic acids (Flower et al. 1996). Allochthonous provision of humic acids can provide essential resources to lakes. The decline in *S. exiguiformis* may be indicative of Lake Yuhuang Chi becoming less dystrophic, perhaps due to less dissolved organic matter being transported into the lake. Zhou et al. (2010) demonstrate a shift from deciduous-conifer mixed forest to steppe forest from elsewhere in the Qinling Mountains, especially after 2,900 cal yrs BP, which will have altered catchment – lake dynamics and the transport of allochthonous material. This coincides with breakpoints for both high guild (guild 2) and motile (guild 3) diatoms (Table 2), which may be related to the provision of resources linked to catchment changes around the lake.

The number of limiting resources has a defining influence on community composition. In aquatic environments, when the number of limiting resources increases during times of environmental stress, deterministic processes become more important in structuring communities, leading to a decline in beta-diversity (Chase 2010; Larson et al. 2016). Initially, beta-diversity between 3,500 – 3,100 cal yrs BP does not decline (Fig 3), which suggests

that at the start of our record, diatoms were able to adapt to changing resources, such that resources were not limiting. The presence of *H. schmassmannii* (a motile diatom) in alpine and arctic lakes is linked to relatively low levels of DOC (Buczkó et al. 2015). In Lake Yuhuang Chi, therefore, the initial increase of this species suggests that it replacing *S. exiguiformis* as resources into the lake changed. The decline in this species after c. 2800 cal yrs BP tracks the switch to steppe forest (Zhou et al. 2010) and the progressively cooler and more arid climate (Wang et al. 2005; Chen et al. 2015b). Declining beta-diversity (especially during the latter stages of zone 1, after 2,800 cal yrs BP), suggests that as regional temperatures cooled and aridity increased (Chen et al. 2015a), resources became more limiting (Fig 6a).

However, there were periods when the availability of resources stabilised or even increased slightly during the neoglacial, e.g. between c. 2,000 – 1,400 cal yrs BP (Fig 6a). This period coincides with distinctly warmer Arctic and European temperatures (PAGES 2k Consortium 2013), commonly referred to as the 'Roman Warm Period', although in eastern China temperatures declined, especially due to strong winter temperature anomalies (Ge et al. 2003). Strong seasonality at this time therefore likely affected resource availability, given that high profile diatoms dominate the assemblage, and exhibit a significant breakpoint at c. 1565 cal yrs BP (Table 2; Fig 4).

Figure 6: Beta-diversity here is plotted alongside internal and external climate forcings: mean temperature stack records for low latitude temperature anomalies (Fig 7b; Marcott et al. 2013); Chinese winter temperature anomalies (Fig 7c; Ge et al. 2003); trends in pollen-inferred mean annual precipitation (Fig 7d; Chen et al. 2015a); K+ concentrations in the GISP ice core (Fig 7e; Mayewski et al. 2004); sun spot numbers (Fig 7f; Solanki et al. 2004); June solar insolation at 30 N (W m^{-2}) (Fig 7g; Berger & Loutre 1991)

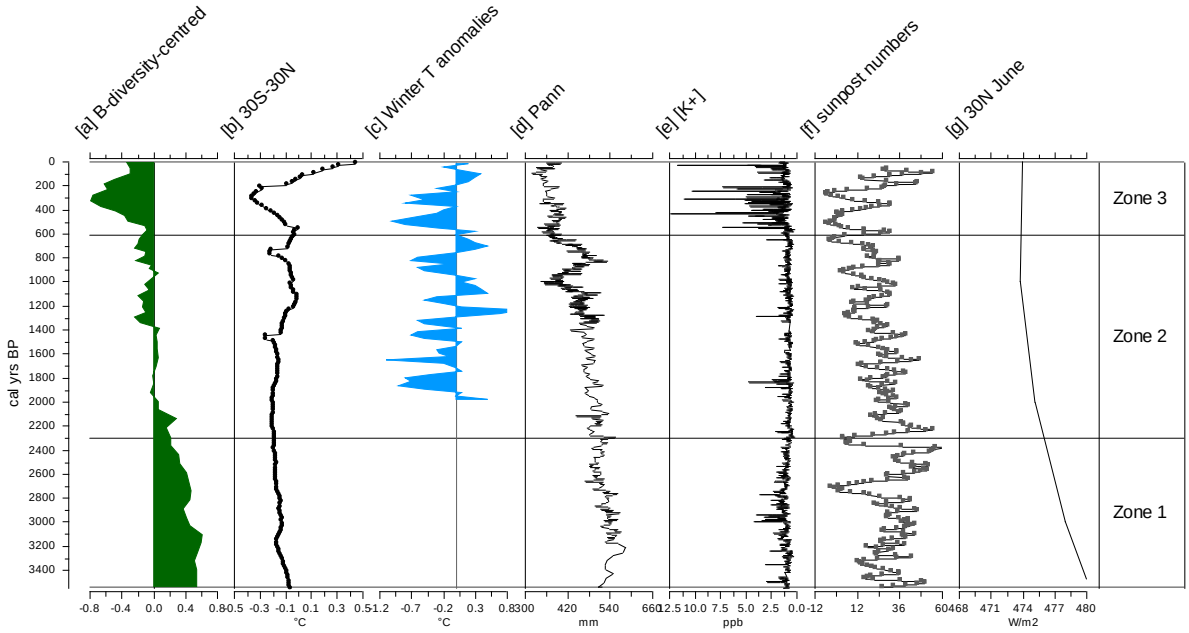

Between 1400 – 615 cal yrs BP (550 - 1335 CE), beta-diversity was lower than average (Fig 6a), and quite variable. Temperature reconstructions from over 200 tree-ring records in Asia reveal a period of greater warmth than the following four centuries (PAGES 2k Consortium 2013), including central China (Ge et al. 2003) (Fig 6c). Precipitation in central China is closely tied to the intensity of the Asian summer monsoon (ASM) (Chen et al. 2015a), and monsoon strength showed distinct variability, being higher in central (Paulsen et al. 2003; Chen et al. 2015b; Wang et al. 2016) and north east China (Chen et al. 2015a,b) than north west China (Chen et al. 2015b). This period coincides with the Medieval Climactic Anomaly (MCA), sometimes referred to the Medieval Warm Period. Sub-decadal isotopic records from a stalagmite from Buddha cave in the Qinling Mountains indicate a period of warm, wet climate between c. 985 – 475 cal yrs BP (965 – 1475 CE) (Paulsen et al. 2003),

while phenology records from the Yellow and Yangtze rivers show that winter half-year temperatures were high between 1380 – 640 cal yrs BP (570 – 1310 CE) (Ge et al. 2003; Fig 6c). A recent palaeolimnological investigation from another alpine lake on Taibai Mountain, Lake Sanqing Chi, inferred warm, wet conditions due to increased presence of *Quercus* and *Betula* pollen (Wang et al. 2016), while Li et al. 2005 used pollen evidence to show that the warmest period in the late Holocene on Tabai mountain occurred between 520 – 1220 CE, with temperatures perhaps being as much as 2 °C warmer than mean annual temperatures observed today.

In oligotrophic lakes, growth of the planktic diatom *P. bodanica* is related to increased mixing depth (Saros & Anderson 2015), because it can tolerate relatively low light levels and take advantage of increased nutrient availability (Malik & Saros 2016). Increasing diatom flux at Lake Yuhuang Chi between c. 1500 - 800 cal yrs BP (450 – 1150 CE) (driven mainly by increasing *P. bodanica*), likely reflects shorter ice duration, with enhanced overturn, driven by increased summer monsoon intensity (Chen et al. 2015a). An increase in beta-diversity reflects the decline in the number of resources that are limited. However, these changes at Lake Yuhuang Chi are relatively muted in comparison to the almost complete switch in oligotrophic to eutrophic diatom communities at the high altitude Gonghai Lake (1,840 m.a.s.l.), located to the north west in the Chinese Loess Plateau. Differences are likely due to the altitudinal differences and phosphorus-rich erodible soils of the loess catchment (Liu et al. 2017).

4.2 Abrupt ecological change during centennial-scale cold events

Against a backdrop of low northern hemisphere summer insolation (Fig 6g), amplified by centennial-scale oceanic variability (Renssen *et al.*, 2006), late Holocene cold events were caused by several “overlapping” factors (such as volcanic eruptions and solar minima) (e.g. Wanner *et al.*, 2014). The most recent wide-scale cold event is the period commonly known as the Little Ice Age approximately 1400 – 1850 CE, caused by several interacting, time-

transgressive forcings. It is the cooling event that we focus on in this study, because cluster analyses of diatom assemblages delineate the boundary between zones 2 and 3 at 1335 CE, and beta-diversity significantly declines at this time to lowest values in the whole record by 1615-1620 CE (Fig 3, Fig 6a).

Describing the Little Ice Age as a period characterised by cooler climate and glacier readvance is rather simplistic, but one that has proven quite resilient, even as its complexities are better understood (e.g. Matthews and Briffa 2005). As more regions are investigated, impacts extend to changes in aridity as well as temperature. For example, Chen et al. (2015b) demonstrated that by and large, regions north of 34° latitude (where our study site is located) were generally drier than regions further south, with the extent of aridity being affected by ocean-atmospheric interactions, such as ENSO, and its teleconnections to SE Asia. The LIA is especially characterised by a strengthened Siberian High (SH), a semi-permanent anticyclone centred over Eurasia which strengthens intensively every winter. A strong Siberian High results in a strong East Asian Winter Monsoon (EAWM) (Zhang et al. 1997). K^+ concentrations in the GISP ice core clearly show that the Siberian High was especially strong between 1400 – 1800 CE (Fig 6f; Mayewski et al. 2004). Concurrent with increased aridity, global low latitude temperature records show rapid cooling at this time (Fig 6b; Marcott et al. 2013), which in China led to very low winter anomalies from phenelogical records (Ge et al. 2003) (Fig 6c).

Very low diatom fluxes characterise the past 800 years at Lake Yuhuang Chi (Fig 3), indicative of reduced diatom productivity, linked to prevailing colder climate. During this time, low profile and planktic diatom guilds are relatively the most important they've been for the past 3500 years (Fig 4), indicating that conditions which caused the lake to become oligotrophic 800 years ago, still persist today. However, planktonic diatoms show a distinct decline during the LIA, likely related to extreme cold conditions and extended ice cover on the lake. The disappearance of *S. exiguiformis* from the record may be due to enhanced

frozen soils, leading to the cessation of carbon transport to the lake, while the disappearance of *H. schamassmannii* may be because it cannot tolerate such low water temperatures (Buczkó et al. 2015). The appearance of *Denticula subtilis*, a very motile diatom that can also be an epiphyte commonly found growing on mosses in littoral habitats, may be due to its exploiting a new habitat for the limited resources available. It may also be reflective of the lake becoming more shallow due to increased aridity; precipitation minima were reconstructed from nearby by Gonghai lake (Chen et al. 2015a). At neighbouring Lake Sanqing Chi, pollen frequencies from *Larix* and *Ephedra* are very high, indicative of cold, dry conditions (Wang et al. 2016). Following harshest conditions for diatom growth in Lake Yuhuang Chi in the middle of the 17th century, beta-diversity increases once more, indicative of more resources becoming available, although diatom fluxes overall remain very low. Modern tundra vegetation developed again on Tabai, with the establishment of the modern tree-line (Li et al. 2005).

While cold and arid climate during the LIA had a major impact on diatom diversity in Lake Yuhuang Chi, impacts from previous centennial-scale cold events such as the 2,800 yr BP event, are inconclusive. Like the LIA, the event dated at c. 2,800 yr BP is concurrent with a deep, abrupt reduction in solar activity (Fig 6f), which led to a decline in surface water temperatures in the North Atlantic (Andersson *et al.*, 2003), weaker meridional overturning circulation (Hall *et al*., 2004) and sea-ice expansion (Renssen et al. 2006). But although these events led to a rapid weakening in ASM intensity in southern China (Wang et al. 2005), reconstructed precipitation from Gonghai Lake in northern China suggests that aridity was already declining from c. 3,100 cal yrs BP (Fig 6d) (Chen et al. 2015b). Moreover, there is a distinct difference in GISP2 K^+ concentrations, which suggests that the Siberian High around the time of the did not reach the strengths observed during the LIA (Fig 6e). At Lake Yuhuang Chi, while there are small declines in beta-diversity and total diatom fluxes, these occur c. 3000 cal yrs BP, in line with increasing regional aridity (Chen et al. 2015b). Breakpoints in high profile and motile diatom guilds are detected slightly later at c. 2,900 cal

yrs BP. The difference in expression of these cold events at Lake Yuhuang Chi highlights their uneven impacts globally.

5. Conclusions

Trends in diatom beta-diversity in freshwater ecosystems in the Qinling mountains of central China reflect changing resource availability, linked to both long term, and abrupt, climate change impacts on lakes and their catchments. For example, the overall gradual decline in beta-diversity over the past 3,500 years mirrors declining low latitude June insolation, which drives overall low latitude cooling (Marcott et al. 2013). This suggests a strong link between orbitally-forced climate change and the availability of limiting resources in this biodiversity-rich alpine region. Over the last 1300 years, impacts related to the Medieval Climatic Anomaly and the Little Ice Age are also expressed in palaeolimnological records from Lake Yuhuang Chi. Inferred increased summer precipitation during the MCA from nearby records resulted in increased diatom fluxes, including planktonic species adapted to mixing of deep waters. Colder, more arid conditions during the Little Ice Age period had an impact on freshwater ecosystem dynamics, providing evidence that this alpine region in central China is very sensitive to climate change, caused by both extrinsic and intrinsic factors. Regional warming after the LIA led to more resources being made available to diatoms once more, especially planktonic species, although overall diatom fluxes remain low compared to earlier periods.

6. Acknowledgements:

Funding: The work was supported by a China Scholarship Council award to Dr Bo Cheng, and by the National Natural Science Foundation of China (Grants No. 41771208; No. 41790421)

7. References

Andersson C, Risebrobakken B. Jansen E, Dahl SO (2003) Late Holocene surface ocean conditions of the Norwegian Sea (Vøring Plateau). Paleoceanography, 18, 1044, doi:10.1029/2001PA000654

Birks, H.J.B., 2007. Estimating the amount of compositional change in late-Quaternary pollen-stratigraphical data. *Vegetation History and Archaeobotany*, *16*(2-3), pp.197-202.

Blaauw, M (2010): Methods and code for 'classical' age-modelling of radiocarbon sequences. *Quaternary Geochronology*, 5, 512-518

Buytaert, W., Moulds, S., Acosta, L., De Bievre, B., Olmos, C., Villacis, M. Tovar, C. and Verbist, K. M. J. (2017) 'Glacial melt content of water use in the tropical Andes, *Environmental Research Letters*, 12, 114014.

Buczkó, K., Wojtal, A.Z., Beszteri, B. and Magyari, E.K., (2015). Morphology and distribution of Navicula schmassmannii and its transfer to genus Humidophila. *Studia Botanica Hungarica*, *46*(1), pp.25-41.

Chase, J.M., (2010). Drought mediates the importance of stochastic community assembly. *Proceedings of the National Academy of Sciences*, *104*(44), pp.17430-17434.

Chen, F., Xu, Q., Chen, J., Birks, H.J.B., Liu, J., Zhang, S., Jin, L., An, C., Telford, R.J., Cao, X. and Wang, Z., (2015a). East Asian summer monsoon precipitation variability since the last deglaciation. *Scientific Reports*, *5*, p.11186.

Chen, J., Chen, F., Feng, S., Huang, W., Liu, J., Zhou, A. (2015b) Hydroclimatic changes in China and surroundings during the Medieval Climate Anomaly and Little Ice Age: spatial patterns and possible mechanisms. Quaternary Science Reviews 107, 98-111

Cook, E.R., Krusic, P.J., Anchukaitis, K.J., Buckley, B.M., Nakatsuka, T., Sano, M., PAGES Asia2k Members 2013. Tree-ring reconstructed summer temperature anomalies for temperate East Asia since 800 C.E. Climate Dynamics 41, 2957-2972

Cook, E.R., Anchukaitis, K.J., Buckley, B.M., D'Arrigo, R.D., Jacoby, G.C. and Wright, W.E., 2010. Asian monsoon failure and megadrought during the last millennium. *Science*, *328*, pp.486-489.

Fan, J.T., Li, J.S., Xia, R., Hu, L.L., Wu, X.P., Guo, L., (2014). Assessing the impact of climate change on the habitat distribution of the giant panda in the Qinling Mountains of China. Ecol. Model. 274, 12–20.

Flower, R.J., V.J. Jones & F.E. Round. (1996). The distribution and classification of the problematic *Fragilaria* (*virescens* V.) *exigua* Grun./*Fragilaria exiguiformis* (Grun.) Lange-Bertalot: A new species or a new genus? Diatom Research, 11, 41–57.

Ge, Q., Zheng, J., Fang, X., Man, Z., Zhang, Z., Zhang, P., Wnag, W. 2003. Winter half-year temperature reconstruction for the middle and lower reaches of the Yellow River and Yangtze River, China, during the past 2000 years. The Holocene, 13, 933-940

Grêt-Regamey, A., Brunner, S.H. and Kienast, F., 2012. Mountain ecosystem services: who cares?. *Mountain Research and Development*, *32*, pp.S23-S34.

542 Guo, J., Huang, G., Wang, X., Li, Y., Lin, Q. 2017. Investigating future precipitation
543 changes over China through a high-resolution regional climate model ensemble. Earth's
544 Future 5, 285-303.
545
546 Hall IR, Bianchi GG, Evans JR (2004) Centennial to millennial scale Holocene climate-
547 deep water linkage in the North Atlantic. Quaternary Science Reviews, 23, 1529–1536
548
549 Juggins, S., (2017). rioja: Analysis of Quaternary Science Data, R package version
550 3.5.1.(http://cran.r-project.org/package=rioja)
551
552 Krammer, K., Lange-Bertalot, H., (1986). Bacillariophyceae: Naviculaceae. In: Ettl, H.,
553 Gerloff, J., Heynig, H., Mollenhauer, D. (Eds.), Süsswasserflora von Mitteleuropa. Band
554 2, Teil 1. Gustav Fischer, Stuttgart.
555
556 Krammer, K., Lange-Bertalot, H., (1988). Bacillariophyceae: Bacillariaceae,
557 Epithemiaceae, Surirellaceae. In: Ettl, H., Gerloff, J., Heynig, H., Mollenhauer, D. (Eds.),
558 Süsswasserflora von Mitteleuropa. Band 2, Teil 2. Gustav Fischer, Stuttgart.
559
560 Krammer, K., Lange-Bertalot, H., (1991a). Bacillariophyceae: Achnanthaceae, Kritische
561 Erga¨ nzungen zu Navicula (Lineolatae) und Gomphonema Gesamtliterarurverzeichnis.
562 In: Ettl, H., Gerloff, J., Heynig, H., Mollenhauer, D. (Eds.), Süsswasserflora von
563 Mitteleuropa. Band 2, Teil 4. Gustav Fischer, Stuttgart.
564
565 Krammer, K., Lange-Bertalot, H., (1991b). Bacillariophyceae: Centrales, Fragilariaceae,
566 Eunotiaceae. In: Ettl, H., Gerloff, J., Heynig, H., Mollenhauer, D. (Eds.), Süsswasserflora
567 von Mitteleuropa. Band 2, Teil 3. Gustav Fischer, Stuttgart.
568

569 Lange-Bertalot, H., (2001). Diatoms of Europe, Volume 2: *Navicula sensu stricto*. 10
570 genera separated from *Navicula* sensu lato *Frustulia*. In: Lange- Bertalot, H. (Ed.)
571 Diatoms of Europe: diatoms of the European inland waters and comparable habitats.
572 A.R.G. Gantner Verlag K.G., Ruggell, Germany.
573
574 Larson, C.A., Adumatioge, L. and Passy, S.I., (2016). The number of limiting resources
575 in the environment controls the temporal diversity patterns in the algal benthos. *Microbial*
576 *ecology*, *72*, pp.64-69.
577
578 Leprieur, F., Tedesco, P.A., Hugueny, B., Beauchard, O., Dürr, H.H., Brosse, S. &
579 Oberdorff, T. (2011) Partitioning global patterns of freshwater fish beta diversity reveals
580 contrasting signatures of past climate changes. Ecology Letters, 14, 325–334.
581
582 Li, X., Dodson, J., Zhou, J., Wang, S., Sun, Q. (2005). Vegetation and climate variations
583 at Taibai, Qinling Mountains in central China for the last 3500 cal BP. Journal of
584 Integrative Plant Biology 47, 905-916
585
586 Liu, H., Tang, Z., Dai, J., Tang, Y. and Cui, H., (2002). Larch timberline and its
587 development in North China. *Mountain Research and Development*, *22*, 359-367.
588
589 Liu J, Rühland K.M., Chen J., Xu, Y., Chen, S., Chen, Q., Huang, W., Xu, Q., Chen, F.
590 Smol, J.P. (2017). Aerosol-weakened summer monsoons decrease lake fertilization on
591 the Chinese Loess Plateau. Nature Climate Change 7, 190-195.
592
593 Lotter, A.F., Bigler, C., (2000). Do diatoms in the Swiss Alps reflect the length of ice
594 cover. Aquatic Sciences 62, 125-141.
595

596 Mackay, A. W., Bezrukova, E. V., Leng, M. J., Meaney, M., Nunes, A., Piotrowska, N.,
597 Self, A., Shchetnikov, A., Shilland, E., Tarasov, P., Wang, L. & White, D. (2012). Aquatic
598 ecosystem responses to Holocene climate change and biome development in boreal,
599 central Asia. *Quaternary Science Reviews* 41, 119-131
600
601 Malik, H.I. and Saros, J.E., (2016). Effects of temperature, light and nutrients on five
602 *Cyclotella* sensu lato taxa assessed with in situ experiments in arctic lakes. *Journal of*
603 *plankton research*, *38*, 431-442.
604
605 Mann, M.E., Zhang, Z., Rutherford, S., Bradley, R.S., Hughes, M.K., Shindell, D.,
606 Ammann, C., Faluvegi, G. and Ni, F., (2009). Global signatures and dynamical origins of
607 the Little Ice Age and Medieval Climate Anomaly. *Science*, *326*, 1256-1260.
608
609 Marcott SA, Shakun JD, Clark PU, Mix AC (2013) A reconstruction of regional and global
610 temperature for the past 11,300 years. Science, 339, 1198-1201.
611
612 Matthews, J.A. and Briffa, K.R., 2005. The 'Little Ice Age': re-evaluation of an evolving
613 concept. *Geografiska Annaler: Series A, Physical Geography*, *87*, p7-36.
614
615 Mayewski PA, Rohling EE, Stager JC *et al.,* (2004) Holocene climate variability.
616 Quaternary Research, 62, 243**–**255
617
618 Messerli, B., Viviroli, D. and Weingartner, R., (2004). Mountains of the world: vulnerable
619 water towers for the 21st century. *Ambio*, pp.29-34.
620
621 Mori, A.S., Isbell, F. and Seidl, R., (2018). β-Diversity, Community Assembly, and
622 Ecosystem Functioning. Trends in Ecology and Evolution 33, 549-564

Muggeo, V.M.R. (2008) Segmented: An R Package to Fit Regression Models with Broken-Line Relationships. R News, 8, 20-25.

PAGES 2k Consortium, (2013). Continental-scale temperature variability during the past two millennia. Nat. Geosci. 6, 339e346.

Passy, S.I., (2007). Diatom ecological guilds display distinct and predictable behaviour along nutrient and disturbance gradients in running waters. Aquatic Botany 86, 171–178

Paulsen, D.E., Li, H.C. and Ku, T.L., (2003). Climate variability in central China over the last 1270 years revealed by high-resolution stalagmite records. *Quaternary Science Reviews*, *22*, 691-701.

Pepin, N., Bradley, R.S., Diaz, H.F., Baraër, M., Caceres, E.B., Forsythe, N., Fowler, H., Greenwood, G., Hashmi, M.Z., Liu, X.D. and Miller, J.R., (2015). Elevation-dependent warming in mountain regions of the world. *Nature Climate Change*, *5*, 424-430.

Reimer PJ, Bard E, Bayliss A *et al.,* (2013) IntCal13 and Marine13 radiocarbon age calibration curves 0–50,000 years cal BP. Radiocarbon, 55, 1869–1887.

Renssen, H., Goosse, H. and Muscheler, R., (2006). Coupled climate model simulation of Holocene cooling events: oceanic feedback amplifies solar forcing. *Climate of the Past*, *2*, 79-90.

Rimet, F., Bouchez, A., (2012). Life-forms, cell-sizes and ecological guilds of diatoms in European rivers. Knowl. Manag. Aquat. Ecosyst. 406, 01.

651 Saros, J.E. and Anderson, N.J., (2015). The ecology of the planktonic diatom *Cyclotella*
652 and its implications for global environmental change studies. *Biological Reviews*, *90*,
653 522-541.
654
655 Schmidt, R., Kamenik, C., Lange-Bertalot, H., Klee, R., (2004). *Fragilaria* and *Staurosira*
656 (Bacillariophyceaea) from sediment surfaces of 40 lakes in the Austrian Alps in relation
657 to environmental variables, and their potential for palaeoclimatology. Journal of
658 Limnology 63, 171–189.
659
660 Solanki SK, Usoskin IG, Kromer B, Sch€ussler M, Beer J (2004) An unusually active sun
661 during recent decades compared to the previous 11,000 years. Nature, 431, 1084–1087.
662
663 Šmilauer, P. and Lepš, J., 2014. *Multivariate analysis of ecological data using CANOCO*
664 *5*. Cambridge University Press.
665
666 Smol, J.P., Wolfe, A.P., Birks, H.J.B., and others (2005). Climate-driven regime shifts in
667 the biological communities of arctic lakes. *Proceedings of the National Academy of*
668 *Sciences*, *102*(12), pp.4397-4402.
669
670 Tan, L., Cai, Y., An, Z., Yi, L., Zhang, H. and Qin, S., (2011). Climate patterns in north
671 central China during the last 1800 yr and their possible driving force. *Climate of the*
672 *Past*, *7*, 685-692.
673
674 Tan, L., Cai, Y., Cheng, H., Edwards, E.R., Gao, Y., Xu, H., Zhang, H., An, Z. (2018)
675 Centennial- to decadal-scale monsoon precipitation variations in the upper Hanjiang
676 River region, China over the past 6650 years. Earth and Planetary Science Letters 482,
677 580-590.
678

679 Wang, Y., Cheng, H., Edwards, R.L., He, Y., Kong, X., An, Z., Wu, J., Kelly, M.J.,
680 Dykoski, C.A. and Li, X., (2005). The Holocene Asian monsoon: links to solar changes
681 and North Atlantic climate. *Science*, *308*, 854-857.
682
683 Wang, H., Song, Y. Cheng, Y., Luo, Y., Gao, Y., Deng, L. & Liu, H. (2016) Mineral
684 magnetism and other characteristics of sediments from a sub-alpine lake (3080 m asl) in
685 central east China and their implications on environmental changes for the last 5770
686 years. *Earth and Planetary Science Letters* 452, 44-59.
687
688 Wanner H, Mercolli L, Grosjean M, Ritz SP (2014) Holocene climate variability and
689 change: a database review. Journal of Geological Society of London, 172, 254-263.
690
691 Williams, D.M., Round, F.E., (1987). Revision of the genus *Fragilaria*. Diatom Research
692 2, 267-288.
693
694 Yan, L., Liu, X. (2014). Has climatic warming over the Tibetan Plateau paused or
695 continued in recent years? Journal of Earth, Ocean and Atmospheric Sciences 1, 13-28
696
697 Yang, W., Yan, Y., Zhang, Y., Guo, W. and Zha, F., (2018). Geoheritages in the Qinling
698 Orogenic Belt of China: Features and comparative analyses. *Geological Journal*, *53*, 98-
699 413.
700
701 Zhang, Y., K. R. Sperber, and J. S. Boyle, (1997) Climatology and interannual variation
702 of the east Asian winter monsoon: Results from the 1979–95 NCEP/NCAR reanalysis.
703 Mon. Wea. Rev., 125, 2605–2619
704

Zhang, Y.B., Wang, Y.Z., Phillips, N., Ma, K.P., Li, J.S. and Wang, W., (2017). Integrated maps of biodiversity in the Qinling Mountains of China for expanding protected areas. *Biological Conservation*, *210*, 64-71.

Zhou, A., Sun, H., Chen, F., Zhao, Y., An, C., Dong, G., Wang, Z., Chen, J., (2010). High-resolution climate change in mid-late Holocene on Tianchi Lake, Liupan Mountain in the Loess Plateau in central China and its significance. *Chinese Science Bulletin*, *55*, 2118-2121.

714

715 **Figure Legends**

716

717 Figure 1: Regional position of Lake Yuhuang Chi in the Qinling Mountains of central Asia.
718 The lake is situated 3365m asl, and was formed by glacial activity. The photograph of the
719 frozen lake to the right shows the small catchment and tundra vegetation.

720

721 Figure 2: The age model determined on 5 radiocarbon dates of organic bulk sediments from
722 core YHC15A. The age-depth model was developed with smooth fitting using CLAM 2.2
723 (Blaauw, 2010).

724

725 Figure 3: Diatoms shown greater than 3% in more than one sample. Diatom species are
726 given as relative abundances. Also shown are PCA axes 1 scores for species and genera,
727 beta-diversity values, planktonic-benthic (P/B) ratio data, and mean-centred diatom fluxes.
728 Zones were delimited using CONISS – see text for details. Red arrows delineate important
729 breakpoints in data (where $p<0.001$).

730

731 Figure 4: All diatoms were classified into one of four guilds (after Passy 2007, and Rimet &
732 Bouchez 2012): low profile (guild 1), high profile (guild 2), motile (guild 3) and planktic (guild
733 4). Guilds are presented as relative abundances to the left, and deviations around the mean
734 to the right. Red arrows delineate important breakpoints in data (where $p<0.001$).

735

736 Figure 5: Ordination and biodiversity trends shown as deviations around the mean. Red
737 arrows delineate important breakpoints in data (where $p<0.001$).

738

739 Figure 6: Beta-diversity here is plotted alongside internal and external climate forcings:
740 mean temperature stack records for low latitude temperature anomalies (Fig 7b; Marcott et
741 al. 2013); Chinese winter temperature anomalies (Fig 7c; Ge et al. 2003); trends in pollen-

742 inferred mean annual precipitation (Fig 7d; Chen et al. 2015a); K+ concentrations in the
743 GISP ice core (Fig 7e; Mayewski et al. 2004); sun spot numbers (Fig 7f; Solanki et al. 2004);
744 June solar insolation at 30 N (W m^{-2}) (Fig 7g; Berger & Loutre 1991)
745
746
747